# Supplementary Information

## Table of Contents:



## Materials and Methods

### Cell culture

Primary HUVEC cells (Lonza) were cultured in full EGM2 media. For time course experiments, cells at less than six passages were cultured overnight in EGM2 with 0.5% FBS and then stimulated with 50 μg/ml VEGF (R&D Systems) for 0, 1, 4 and 12 hours. For siRNA transfection, EP300 or control siRNAs (Suppl. Table 4) were transfected into HUVEC cells using siLentFectTM Lipid (Bio-Rad). Experiments were performed 48 hours after siRNA transfection. C646 (Calbiochem) was added to cells at 10 μg/ml 30min before addition of VEGF.

### Chromatin immunoprecipitation:

HUVEC cells were crosslinked with 1% formaldehyde for 10 min at room temperature. Crosslinking was stopped by glycine to 0.125 M. Subsequent steps for chromatin preparation were performed at 4°C as described previously(Lee et al. 2006), with modifications. Nuclei from 5 x $10^7$ cells were extracted with nuclear extraction buffer (20 mM Hepes-KOH pH 7.5, 10 mM KCl, 1 mM EDTA, 0.2% NP40, 1 mM DTT and 10% glycerol) and resuspended in 1 ml sonication buffer (20 mM Tris-HCl pH 8, 150 mM NaCl, 2 mM EDTA, 0.1% SDS, 1% Triton X-100). The extracted nuclei were sonicated using a Misonix Sonicator 3000 (28 cycles, consisting of a 15 second pulse at amplitude 70 followed by 1 min rest). After sonication, insoluble material was removed by centrifugation at 12000xg for 15 min.

Chromatin immunoprecipitation was performed by incubating sonicated chromatin, pre-cleared with 50 µl proteinase A dynabeads (Invitrogen), with 10 µg ChIP antibodies (Suppl. Table 3) overnight at 4°C. Next, antibody-bound chromatin was pulled down using 100 µl BSA-blocked Proteinase A or G dynabeads were added to each sample (A or G were selected based on the antibody species of origin). Beads were washed five times with RIPA buffer (50 mM Hepes-KOH pH 7.5, 500 mM LiCl, 1 mM EDTA, 1% NP40 and 0.7% Na-Deoxycholate) using a magnetic stand. For MED1 and MED12 ChIP, protein G dynabeads were washed once with sonication buffer, once with high salt buffer (20 mM Tris-HCl pH 8, 500 mM NaCl, 2 mM EDTA, 0.1%, SDS, 1% Triton X-100), once with LiCl Buffer (10 mM Tris-HCl pH 8, 250 nM LiCl, 2mM EDTA, 1% NP40) and once with 10mM Tris-HCl pH 8, 10 mM EDTA, and 50 mM NaCl. Precipitated DNA was de-crosslinked at 65°C overnight, treated with 10 µg RNase A and 15 µg proteinase K, and then purified using the Qiagen Min-elute PCR Purification kit.

### Chip-qPCR

ChIP and input DNA sample were amplified with SYBR@ master mix (Life Technologies, USA) on an ABI7500 cycler. ChIP enrichment was calculated by normalization with input and unbound control regions as described previously (He and Pu 2010). Primers used for ChIP-qPCR are listed in Suppl. Table 4. Primers for validation of MED1/12 ChIP in murine ES cells were described previously(Kagey et al. 2010).

### ChIP-seq

Chip-Seq library construction were performed with NEBNext DNA Sample Prep Reagent Set 1 (E6000) using the protocol and reagent concentrations described in the Illumina Mutiplex ChIP-Seq DNA Sample Prep Kit. Libraries were indexed using a single indexed PCR primer (Suppl. Table 4) in place of the dual multiplex Primer 2.0/indexed primers described in the final PCR step of the Illumina protocol. ChIP library size was checked by using an Agilent bioanalyzer, and the functional cluster concentration of each library was determined by qPCR. Libraries were sequenced using a HiSeq 2000 (Illumina) instrument to generate 50 nt single end data. ChIP-seq data for GM12878 were from obtained from wgEncodeEH001487; ref. _(Reddy et al. 2012).

### mRNA-seq

Total RNA of VEGF-treated and non-treated HUVEC cells were isolated with the Qiagen RNeasy mini kit, including on column DNaseI digestion. mRNA selection and library construction was performed as described (Christodoulou et al. 2011), without the library normalization steps. The final PCR amplification was performed with the indexing primers listed in Suppl. Table 4 in place of the dual PCR primer 2.0/indexing primers described in the published protocol. Pair-end, 50 nt sequences were generated on a HiSeq 2000 (Illumina).

### DNase-seq

DNase-seq was performed as described previously (Song and Crawford 2010), with minor modification to permit multiplexing. $3X10^7$ HUVEC cells were collected at 0, 1, 4 and 12 hour after VEGF stimulation, washed with cold PBS, suspended into FBS with 10% DMSO, and stored at -80°C prior to subsequent processing. For DNase digestion, nuclei were isolated from thawed cells and treated with DNase I as described(Song and Crawford 2010). DNA nicks were end repaired and ligated with biotin-labeled DNS linker 1. MmeI digestion released 20bp chromatin DNA afixed to the biotinylated primer. These fragments were purified with streptavidin dynabead. DNA linker 2 with barcode (Suppl. Table 4) was ligated to purified fragments, and the sequencing library was amplified with high fidelity PCR. Libraries were sequenced on an Illumina HiSeq 2000 (50 nt, single end) using a custom library sequencing primer (Suppl. Table 4). Duplicate samples showed high correlation, and replicate 1 was used for the main analysis.

### Immunoprecipitation and Western Blotting

To pull down mediator proteins in the HUVEC and murine ES cells, 1 mg soluble protein was incubated with 3 µg MED1 or MED12 antibody (Suppl. Table 3) overnight at 4 °C. Antibody complexes were then pulled down on Protein A dynabeads, pre-blocked with 1% BSA, for 4 hours at 4°C. After washing, proteins were eluted in 1X Laemmli buffer. Western blotting was performed using standard methods.

### Chromatin Conformation Capture (3C)

Chromatin Conformation Capture was performed essentially as described(Hagege et al. 2007; Xu et al. 2010). $1x10^7$ HUVEC cells treated with 50 µg/ml VEGF for 0, 1, 4 and 12 hours were crosslinked with 2% formaldehyde for 8 min at room temperature on dish. Nuclei were extracted with nuclear extraction buffer and digested with 1000 U EcoRI overnight on a shaking platform. The digested nuclei were ligated with 100 Weiss units of T4 ligase at 16°C for 4 hours in 7 ml 1X ligation buffer. Digestion efficiency was measured using quantitative PCR to compare aliquots taken before and after digestion. Samples with less than 70% complete digestion were discarded. BAC clones (20 µg) containing *KDR* (Invitrogen, clone CTD-2506A13), *CD34* (CHORI, clone RP11-351B8), *DUSP5* (CHORI, clone RP11-108I5) and *VWF* (CHORI, clone RP11-1137J12) were digested with EcoRI and religated to generate control template. Ligation products were measured by quantitative Taqman PCR using primers and probes indicated in Suppl. Table 4. Normalized crosslink frequency was calculated as described(Hagege et al. 2007).

## Enhancer/promoter transcriptional activity assay

1-2 kb regions centered on EP300 binding sites nearest H3K27ac dynamic regions were amplified with *LA Taq* DNA Polymerase (Takara) and inserted into pGL4.11[luc2P] (promoter) or pGL4.24[luc2P/minP] (Enhancer) vectors (Promega, USA) by Gateway recombination (Invitrogen). HUVEC seeded on 24 well plates were then cotransfected with luciferase reporter and internal control (pGL4.74[hRluc/TK] (Promega, USA) plasmids using Lipofectamine LTX (Invitrogen, USA). One day after transfection, cells were serum-depleted overnight and then stimulated with VEGF. Luciferase activity was measured using a 1420 Multilabel Counter (PerkinElmer, USA) after adding Dual-Luciferase Assay substrate (Promega, USA).

## Data Analysis

**ChIP-seq and DNase-seq Read Alignment.** All samples were aligned against hg19 using Bowtie 1.3(Langmead et al. 2009) with the –m 1 switch to only recover uniquely mapping reads. Each set of aligned reads were read into R via the package SPP(Kharchenko et al. 2008) and then filtered for quality using the function remove.local.tag.anomalies. All analyses below were then performed on the filtered read set .

**EP300 Peak Calls.** Using SPP(Kharchenko et al. 2008) on the processed EP300 ChIP-seq data (rep 1), peaks were called using find.binding.positions with a window half size of 120 and a FDR of 1%.

**H3K27ac variance scores and temporal clusters.** To calculate H3K27ac variance scores, the entire genome was divided into 200 bp windows at 50 bp intervals. At each time point, H3K27ac reads were shifted by 73 bp and mapped to bins. For bins containing at least one read, the enrichment was calculated by normalizing it against similarly binned input. The variance score of each bin was calculated as variance(bins over time)/mean (bins over time). A EP300-associated H3K27ac site was defined as the bin ± 2kb from the center of a EP300 site that had the greatest variance score and a mean value of greater than or equal to 3. The subset of EP300-associated H3K27ac with highest variance scores (top 20 percentile) were defined as dynamic, EP300-associated H3K27ac sites and were used for further analysis.

H3K27ac clusters were determined using the dynamic, EP300-associated H3K27ac sites. The variance score of each site was row-scaled across time using a standard normal distribution, then grouped by Hierarchical clustering with average linkage and Ward's method. The top three clusters from the resulting dendrogram were designated H1, H4-12, and H0 based on the temporal pattern of H3K27ac variance score (Suppl. Table 1).

**Functional strand clustering.** To assess whether the H3K27ac and p300 had asymmetric patterns around our variant peak centers, we carried out the functional strand clustering method as described by Kundaje et al. (2012), with some modifications. For each variant cluster, we took the tag density matrix around H3K27ac peaks for both H3K27ac and p300 signal across all four time points. In order to capture patterns across time points and factors, we joined the

H3K27ac and p300 matrixes so that each row represented these signals in the 4 kb centered on the variant site center, across all 4 time points. After creating this joint matrix, we filtered out rows that had a mean signal in the 1st percentile of all rows. After this filtering, we clustered the matrix with k-means clustering, starting with 40 clusters. We then progressively merged similar clusters by their Pearson correlation distance between the cluster means, calculated from all the rows in the cluster from the joint matrix. At each step, the two clusters with the value that minimized the 1-Pearson correlation were merged together. If flipping a cluster's orientation reduced the Pearson correlation distance and led to merger of two clusters, then the cluster was flipped by reversing the orientation of each constituent matrices and then rejoining them in a new joint matrix. This procedure was reiterated until no cluster had a 1-Pearson correlation value less than or equal to .25. After this process, each remaining cluster was then oriented such that the strongest mean signal in the cluster was on the right side of the image.

**Assigning Functional Annotations to Dynamic, p-300 associated H3K27ac Clusters.** The position of each site in the H1, H4-12, and H0 clusters was analyzed using GREAT(McLean et al. 2010). Peaks were associated with the nearest gene within 100 kb. Selected entries from the top 20 significant terms from the Biological Process table are shown in Fig. 4c.

**Tag Aggregation Plots and Heatmaps.** Reads within 3 kb of a feature of interest (either a EP300-associated H3K27ac site, or a peak, as indicated) were binned into 10 bp bins. The aggregation plots were generated by taking the 5% trimmed mean of each bin and normalizing against the mapped library size. For all data sets except DHS, this value was then subtracted against a similarly prepared input matrix. The resulting curve was smoothing using loess smoothing and then plotted. The tag density heatmaps were generated by producing a matrix from the 50 bp binned sites centered on H3K27ac variants, normalizing against the number of mapped reads. The matrix of normalized tag number was log2 transformed and visualized using JavaTreeView (Saldanha 2004).

**mRNA-seq Analysis.** The paired end RNA-seq reads were aligned to Ensembl transcript annotation using Cufflinks 1.3.0(Trapnell et al. 2010) to give gene expression values, expressed as fragments per thousand nt transcript per million reads (FPKM). Each individual RNA-seq sample was initially independently aligned against the Ensembl transcript annotation. Then Cuffdiff was used to identify differentially expressed genes. The time series option was used (-T) to direct Cuffdiff to compare a sample only against the next sample in the series. To generate the heat map of differentially expressed genes, the z-score for each differentially expressed gene was calculated across the time course. These were then clustered by hierarchical clustering using Euclidean distance and Ward's method.

**DHS data analysis.** DHS raw sequence reads were separated by their barcode and the adaptor sequence was removed with Btrim(Kong 2011). The reads without genomic inserts were discarded. The remain sequences were then

aligned to hg19 using Bowtie2, with Strata selected. About 70% of reads were uniquely mapped.

**De novo Motif Discovery**. The central 100 bp of each EP300 peak associated with a dynamic H3K27ac site was analyzed for over-represented motifs using DREME(Bailey 2011). Discovered motifs were annotated by matching to known motifs in the Jaspar(Portales-Casamar et al. 2010) and Uniprobe(Newburger and Bulyk 2009) databases using TomTom(Gupta et al. 2007).

**Supplementary References**


Bailey TL. 2011. DREME: motif discovery in transcription factor ChIP-seq data. *Bioinformatics* **27**: 1653-1659.

Christodoulou DC, Gorham JM, Herman DS, Seidman JG. 2011. Construction of normalized RNA-seq libraries for next-generation sequencing using the crab duplex-specific nuclease. *Curr Protoc Mol Biol* **Chapter 4**: Unit4.12.

Gupta S, Stamatoyannopoulos JA, Bailey TL, Noble WS. 2007. Quantifying similarity between motifs. *Genome Biol* **8**: R24.

Hagege H, Klous P, Braem C, Splinter E, Dekker J, Cathala G, de Laat W, Forne T. 2007. Quantitative analysis of chromosome conformation capture assays (3C-qPCR). *Nat Protoc* **2**: 1722-1733.

He A, Pu WT. 2010. Genome-wide location analysis by pull down of in vivo biotinylated transcription factors. *Curr Protoc Mol Biol* **Chapter 21**: Unit 21.20.

Kagey MH et al. 2010. Mediator and cohesin connect gene expression and chromatin architecture. *Nature* **467**: 430-435.

Kharchenko PV, Tolstorukov MY, Park PJ. 2008. Design and analysis of ChIP-seq experiments for DNA-binding proteins. *Nat Biotechnol* **26**: 1351-1359.

Kong Y. 2011. Btrim: a fast, lightweight adapter and quality trimming program for next-generation sequencing technologies. *Genomics* **98**: 152-153.

Kundaje A, Kyriazopoulou-Panagiotopoulou S, Libbrecht M, Smith CL, Raha D, Winters EE, Johnson SM, Snyder M, Batzoglou S, Sidow A. 2012. Ubiquitous heterogeneity and asymmetry of the chromatin environment at regulatory elements. *Genome Res* **22**: 1735-1747.

Langmead B, Trapnell C, Pop M, Salzberg SL. 2009. Ultrafast and memory-efficient alignment of short DNA sequences to the human genome. *Genome Biol* **10**: R25.

Lee TI, Johnstone SE, Young RA. 2006. Chromatin immunoprecipitation and microarray-based analysis of protein location. *Nat Protoc* **1**: 729-748.

McLean CY, Bristor D, Hiller M, Clarke SL, Schaar BT, Lowe CB, Wenger AM, Bejerano G. 2010. GREAT improves functional interpretation of cis-regulatory regions. *Nat Biotechnol* **28**: 495-501.

Newburger DE, Bulyk ML. 2009. UniPROBE: an online database of protein binding microarray data on protein-DNA interactions. *Nucleic Acids Res* **37**: D77-82.

Portales-Casamar E, Thongjuea S, Kwon AT, Arenillas D, Zhao X, Valen E, Yusuf D, Lenhard B, Wasserman WW, Sandelin A. 2010. JASPAR 2010: the greatly

expanded open-access database of transcription factor binding profiles. *Nucleic Acids Res* **38**: D105-10.

Reddy TE et al. 2012. Effects of sequence variation on differential allelic transcription factor occupancy and gene expression. *Genome Res* **22**: 860-869.

Saldanha AJ. 2004. Java Treeview--extensible visualization of microarray data. *Bioinformatics* **20**: 3246-3248.

Song L, Crawford GE. 2010. DNase-seq: a high-resolution technique for mapping active gene regulatory elements across the genome from mammalian cells. *Cold Spring Harb Protoc* **2010**: pdb.prot5384.

Trapnell C, Williams BA, Pertea G, Mortazavi A, Kwan G, van Baren MJ, Salzberg SL, Wold BJ, Pachter L. 2010. Transcript assembly and quantification by RNA-Seq reveals unannotated transcripts and isoform switching during cell differentiation. *Nat Biotechnol* **28**: 511-515.

Xu J, Sankaran VG, Ni M, Menne TF, Puram RV, Kim W, Orkin SH. 2010. Transcriptional silencing of {gamma}-globin by BCL11A involves long-range interactions and cooperation with SOX6. *Genes Dev* **24**: 783-798.

**A**

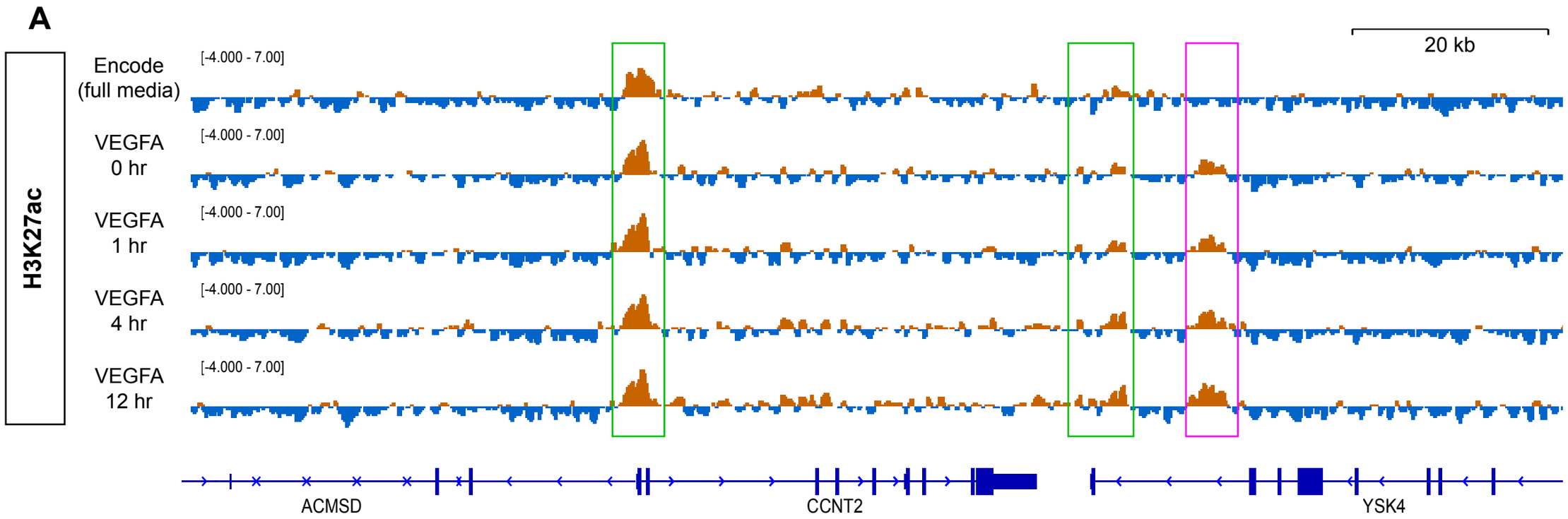


**B**

| | Hour 0 | Hour 1 | Hour 4 | Hour 12 | ENCODE |
|---|---|---|---|---|---|
| **Hour 0** | 1.000 | 0.905 | 0.864 | 0.841 | 0.497 |
| **Hour 1** | 0.905 | 1.000 | 0.882 | 0.858 | 0.480 |
| **Hour 4** | 0.864 | 0.882 | 1.000 | 0.910 | 0.501 |
| **Hour 12** | 0.841 | 0.858 | 0.910 | 1.000 | 0.466 |
| **ENCODE** | 0.497 | 0.480 | 0.501 | 0.466 | 1.000 |

**Suppl. Fig. 1. H3K27ac ChIP-seq data in full media (ENCODE) compared to serum starvation followed by VEGFA stimulation. A.** Representative browser view. Green boxes indicate H3K27ac patterns consistent between our data and ENCODE. Red boxes indicate divergent H3K27ac patterns. **B.** Pearson correlation coefficient between H3K27ac datasets in this study (Hours 0-12) and ENCODE data. Correlation coefficient was calculated by dividing the genome into 200 bp windows.

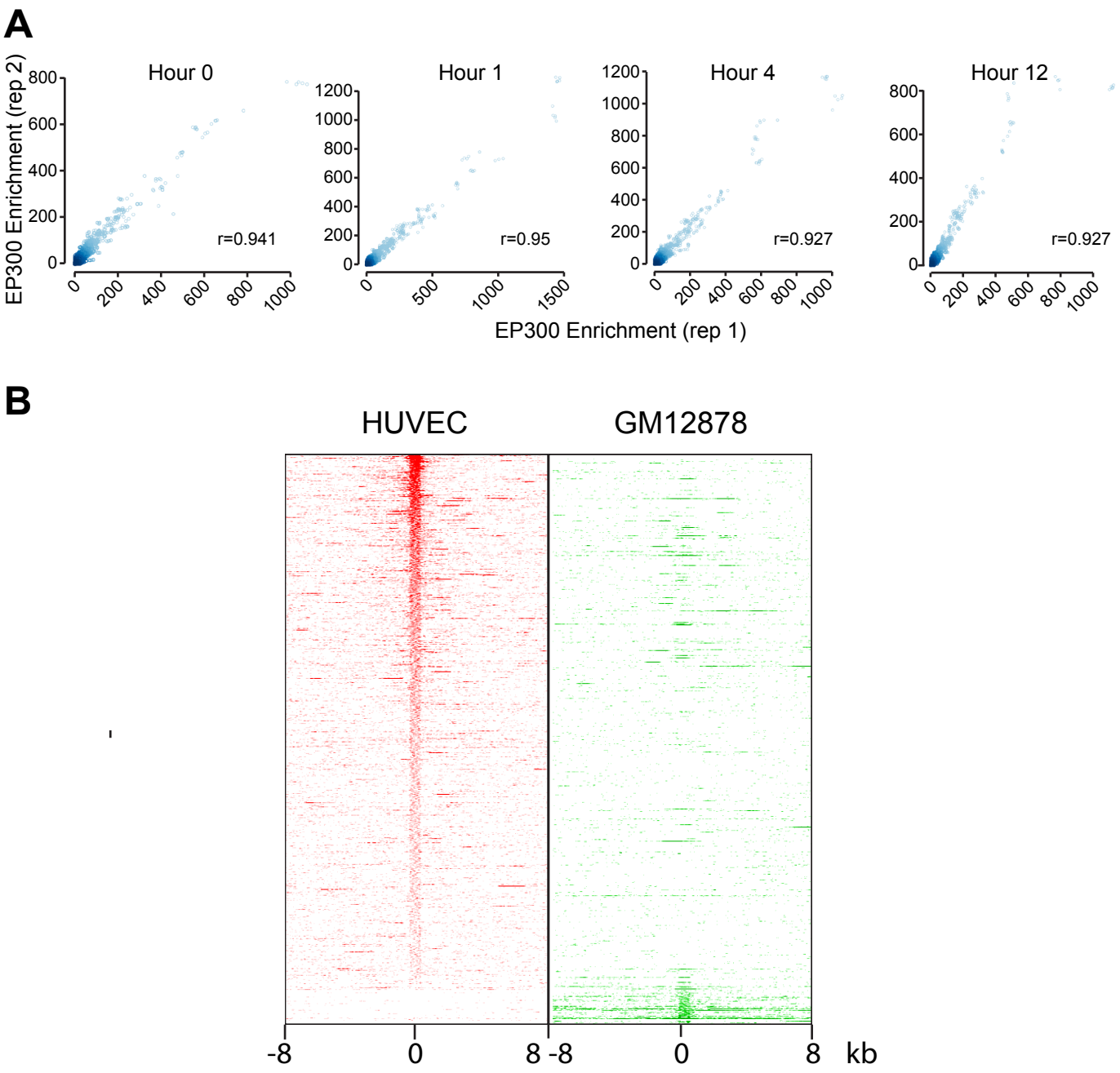


**Suppl. Fig. 2. EP300 chromatin occupancy in HUVEC cells. A.** Correlation between biological replicate EP300 ChIP-seq experiments. **B**. EP300 sites in HUVEC cells compared to GM12878. Rows represent 8 kb regions centered on p300 sites in GM12878 orHUVEC (union of peaks at all VEGFA time points). Few regions of EP300 enrichment were shared between GM12878 and HUVEC.

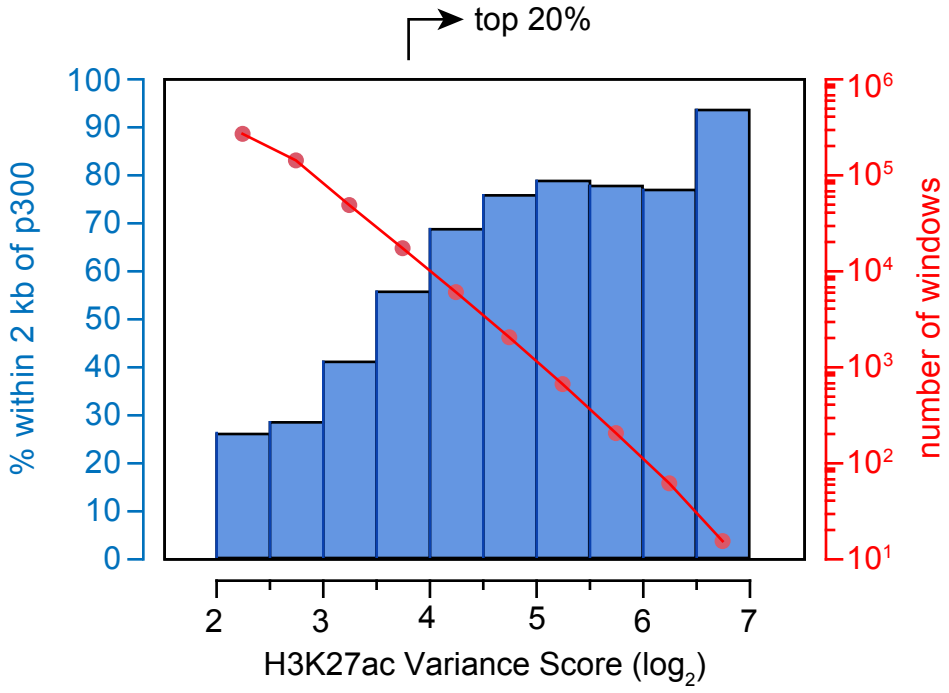


**Suppl. Fig. 3. H3K27ac variance score and frequency of nearby p300 sites.** The variance score of H3K27ac enrichment in 200 bp genomic windows was calculated. The plot shows the number of windows with a given variance score (red) and the frequency of they occur within 2 kb of p300 (blue). The peaks in the top 20th percentile of H3K27ac variance scores are indicated.

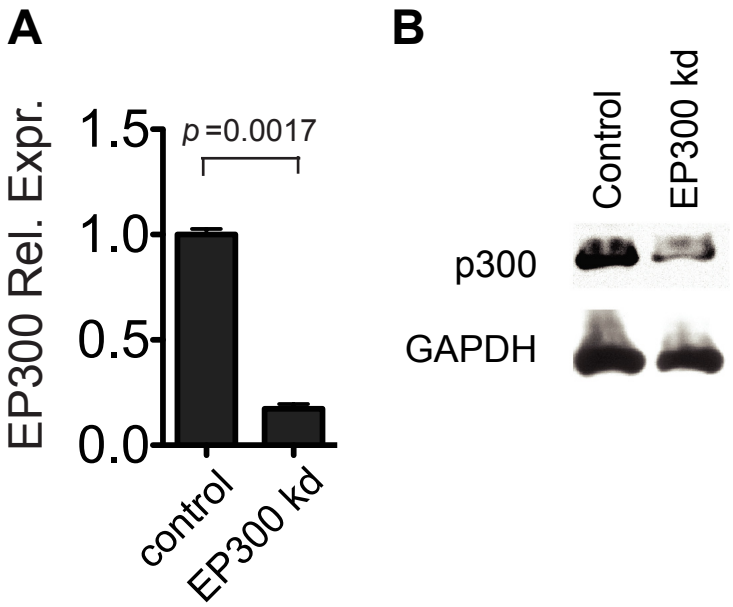


**Suppl. Fig. 4. EP300 knockdown by siRNA.**
HUVEC cells were transfected with siRNA directed against EP300 or control. EP300 RNA and protein were measured by qRTPCR (**A**) or western blotting (**B**).

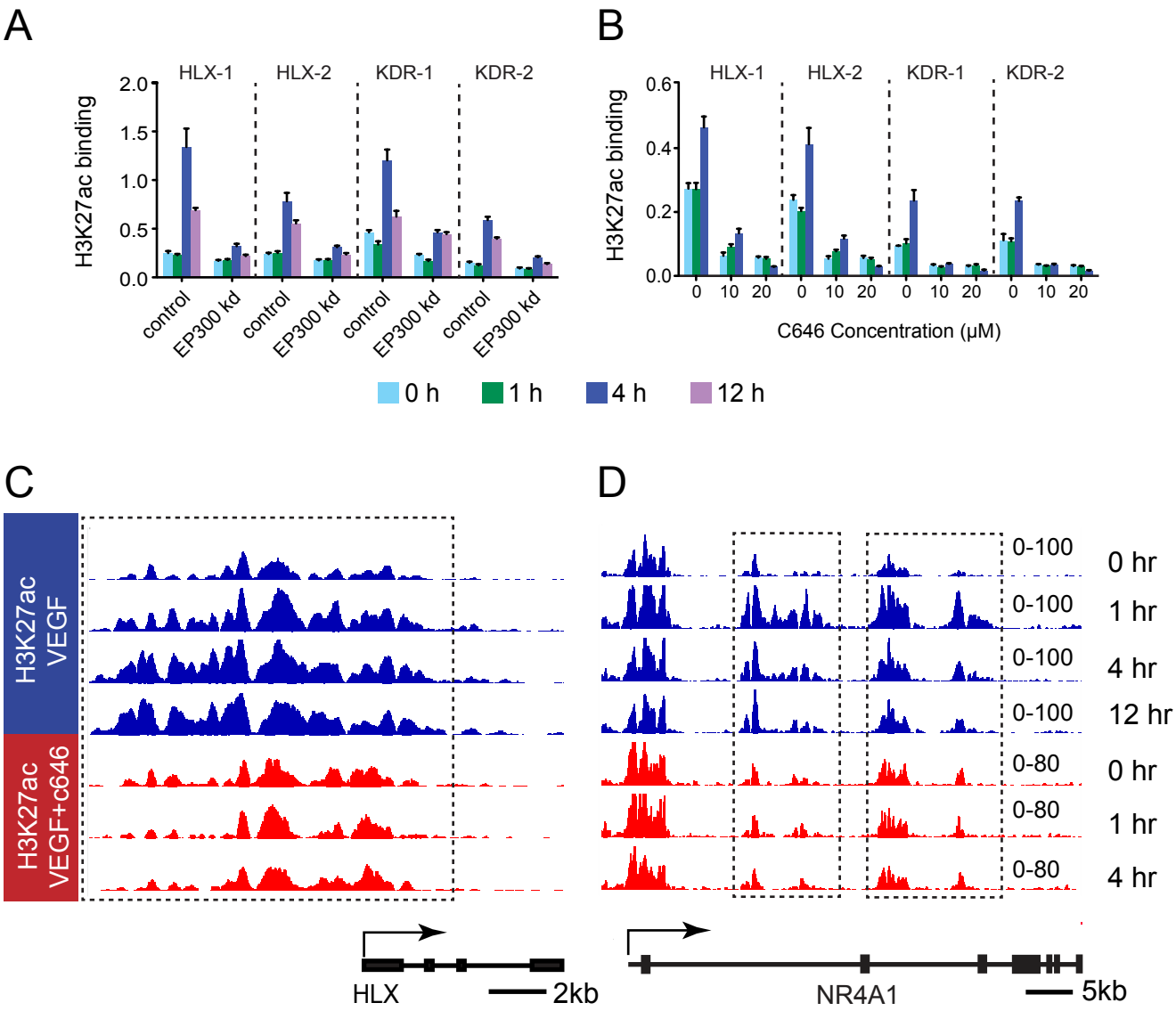


**Suppl. Fig. 5. Inhibition of VEGFA-induced H3K27 acetylation changes by the EP300 inhibition. A.** EP300 siRNA knockdown blunted H3K27ac changes induced by VEGF-A at 4 tested loci (HLX-1, HLX-2, KDR-1, and KDR-2). **B.** EP300 inhibition with the small molecule inhibitor C646 similarly blunted H3K27ac changes induced by VEGF-A at the 4 tested loci. **C-D.** Browser view corresponding to Fig. 1A-B. Dynamic H3K27ac regions are outlined by dotted lines. C646 blunded VEGF-A induced H3K27ac changes.

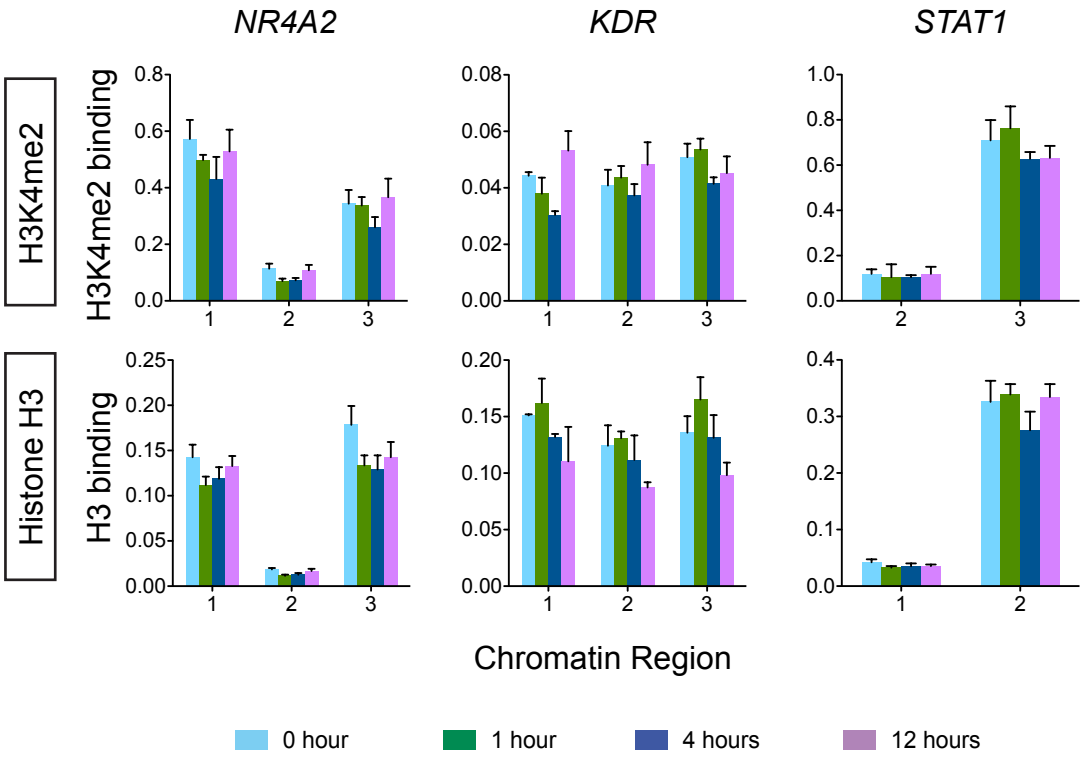


**Suppl. Fig. 6. Chip-qPCR of H3K4me2 and histone H3 binding at dynamic H3K27ac sites.** Numbered chromatin regions are indicated in Fig. 1D.

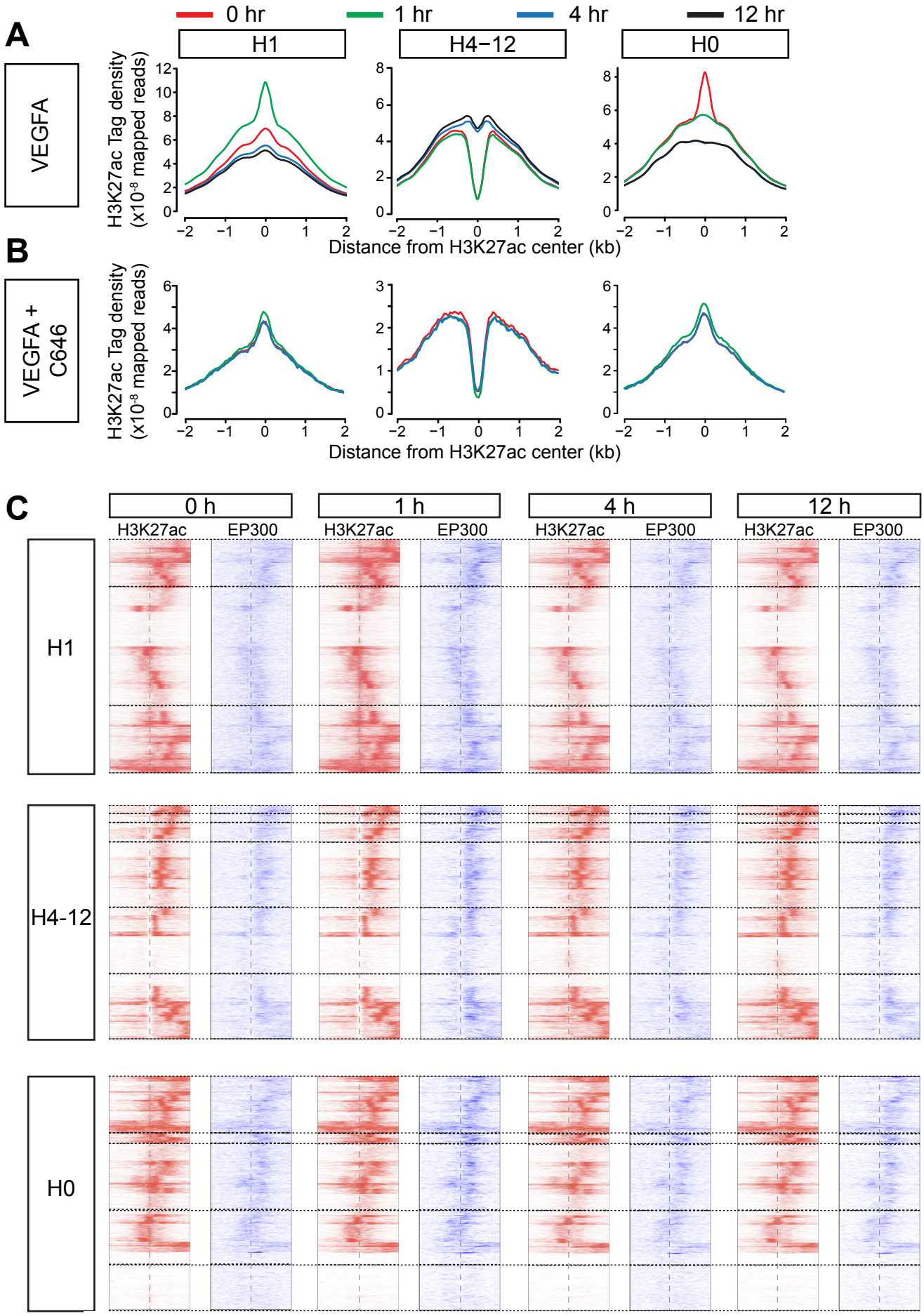
A
VEGFA
0 hr
1 hr
4 hr
12 hr
H1
H4−12
H0
H3K27ac Tag density (x10⁻⁸ mapped reads)
Distance from H3K27ac center (kb)
B
VEGFA + C646
H3K27ac Tag density (x10⁻⁸ mapped reads)
Distance from H3K27ac center (kb)
C
0 h
1 h
4 h
12 h
H3K27ac
EP300
H1
H4-12
H0

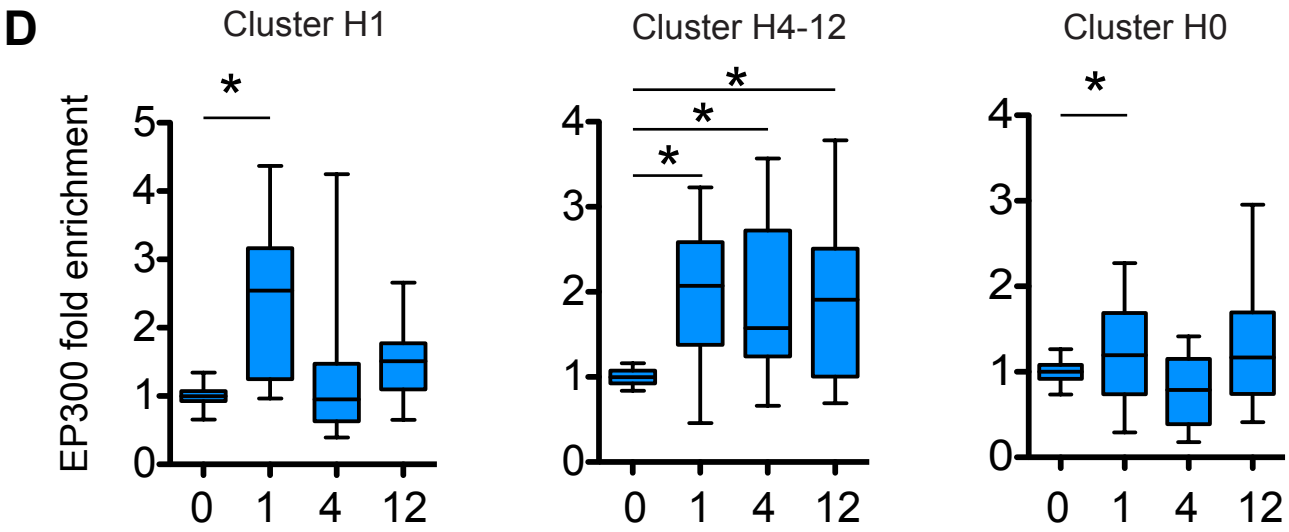


**Suppl. Fig. 7. Dynamic, p300-associated, H3K27ac sites.** These sites are in the top 20% of H3K27ac variance scores and are within 2 kb of p300. Time points indicate number of hours that HUVEC cells were treated with VEGFA, after 12 hours of serum starvation.
**A.** Aggregation plots of H3K27ac tag density in H1, H4-12, and H0 clusters.
**B.** Analogous aggregation plots as in A, but HUVECs were pretreated with EP300 inhibitor C646 prior to VEGFA stimulation. Note loss of VEGFA-induced changes in H3K27ac. C646 samples were collected at 0, 1, and 4 hour, but not 12 hour, timepoints.
**C**. Tag heat maps of H3K27ac enrichment in VEGFA-treated HUVECs, analyzed using an algorithm for functional strand clustering. Horizontal dotted lines indicate demark separate clusters. Vertical dotted lines indicate the center of the dynamic H3K27ac region. Note that H3K27ac enrichment was predominantly asymmetric around the center of the dynamic site.
**D.** Chip-qPCR validation of VEGFA-stimulated EP300 binding. Six different regions within each cluster were measured at each time point. Middle line indicates median, boxes indicate quartiles, and whiskers indicate min/max values. *, $p < 0.05$.

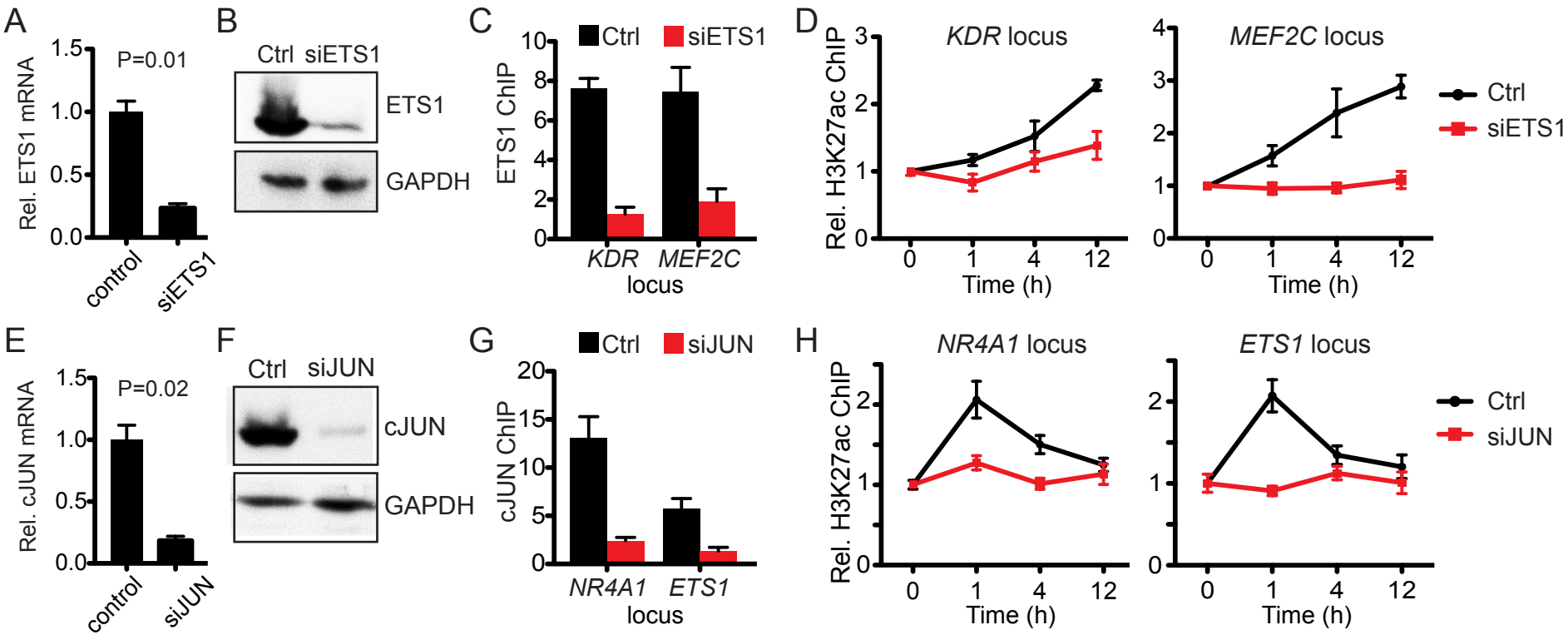


**Suppl. Fig. 8. ETS1 and cJUN promoted H3K27ac changes at tested sites. A-B**. mRNA and protein knockdown of ETS1 by transfection of HUVEC with specific or control siRNA. **C.** Enrichment of ETS1 at loci near *KDR* and *MEF2C* loci in control or siETS1 treated HUVEC. siETS1 reduced ETS1 occupancy ofthese sites. **D.** Relative H3K27ac enrichment at loci near *KDR* and *MEF2C* in control or siETS1 treated HUVEC. siETS1 blocked the increase of H3K27ac at these sites. **E-F.** mRNA and protein knockdown of cJUN by transfection of HUVEC with specific or control siRNA. **G.** Enrichment of cJUN at loci near *NR4A1* and *ETS1* loci in control or siJUN treated HUVEC. siJUN reduced cJUN occupancy of these sites. **H.** Relative H3K27ac enrichment at loci near *NR4A1* and *ETS1* in control or siJUN treated HUVEC. siETS1 blocked the increase of H3K27ac at these sites.

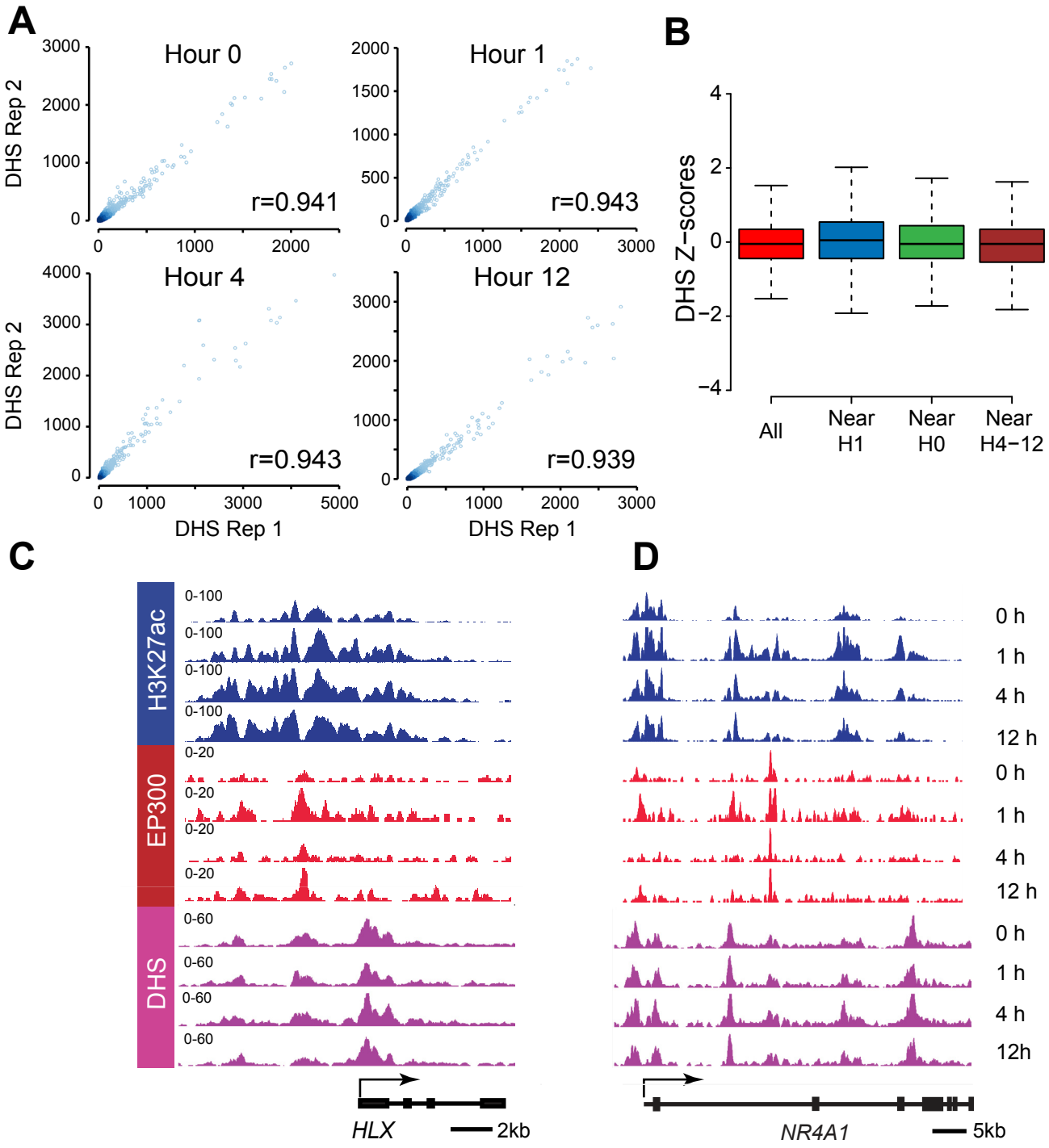


**Suppl. Fig. 9. VEGFA stimulation did not significantly change chromatin accessibility near dynamic, EP300-associated H3K27ac sites.** Chromatin accessibility was measured by sensitivity to DNase I digestion. **A.** Correlation between biological duplicates. **B**. Box plot of DNase-seq variation during the VEGFA stimulation time course, across the genome (All) or within 2 kb of members of H1, H4-12, or H4-12 H3K27ac clusters. DNase-seq reads at each time point during VEGFA stimulation were mapped to 200 bp windows. For each window with a mean of at least 10 reads, the z-score of the var/mean was calculated. Line, box, and whiskers represent the median, 25th and 75th quartiles, and 1.5 times the interquartile distance, respectively. Dynamic H3K27ac sites had no greater change over the time course than unselected DHS sites. **C-D**. Browser images of DHS signal at sites of significant H3K27ac variation. Note that DHS signal did not significantly change during the VEGFA stimulation time course.

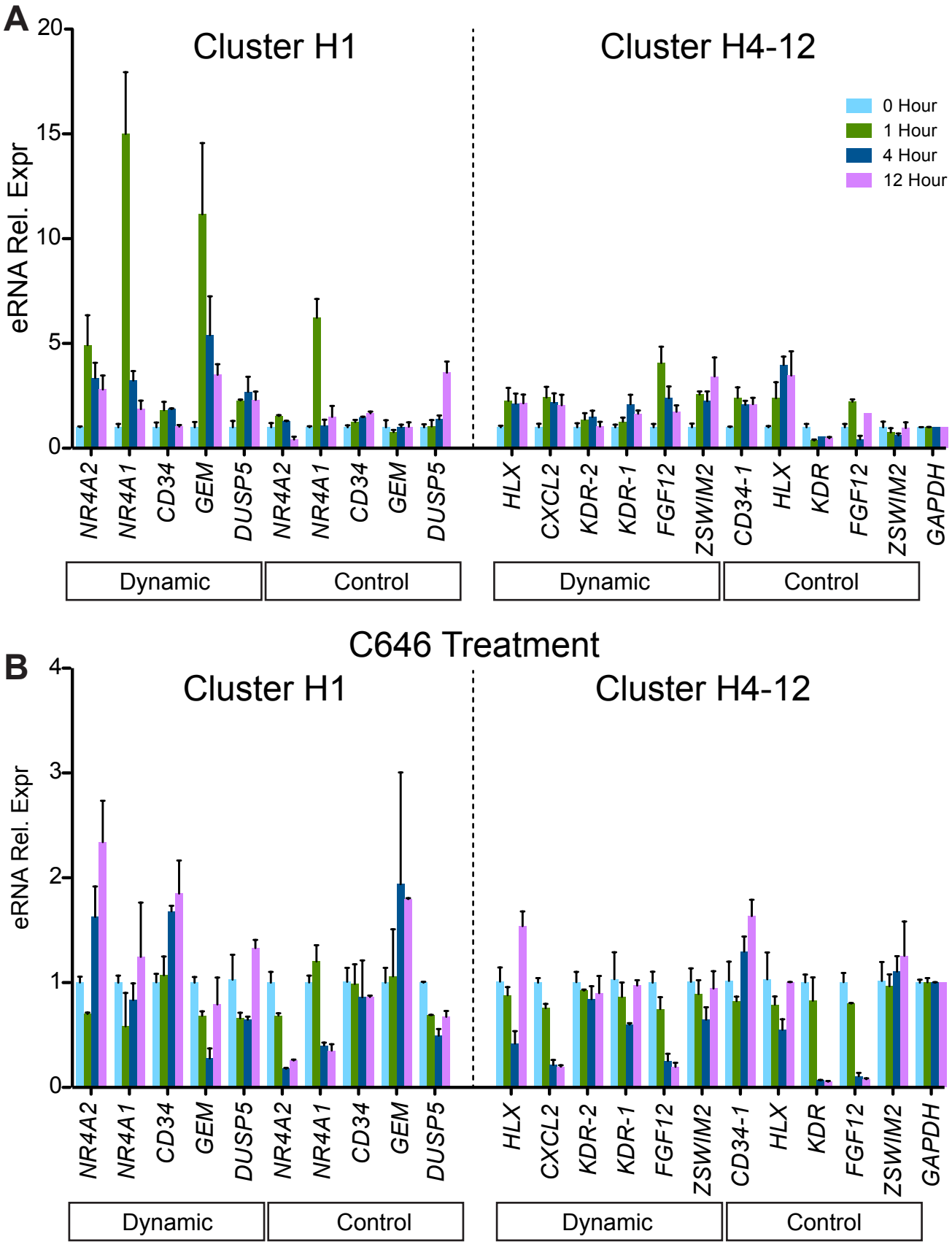


**Suppl. Fig. 10. Dynamic H3K27ac sites expressed VEGFA-responsive eRNA. A**. qRTPCR of eRNA expression at dynamic H3K27ac sites in the H1 or H4-12 clusters. Control indicates nearby regions with H3K27ac that did not score among the most highly variant H3K27ac sites. **B**. qRT-PCR of eRNA expression at the sites studied in (A), in the presence of the EP300 acetyltransferase inhibitor C646.

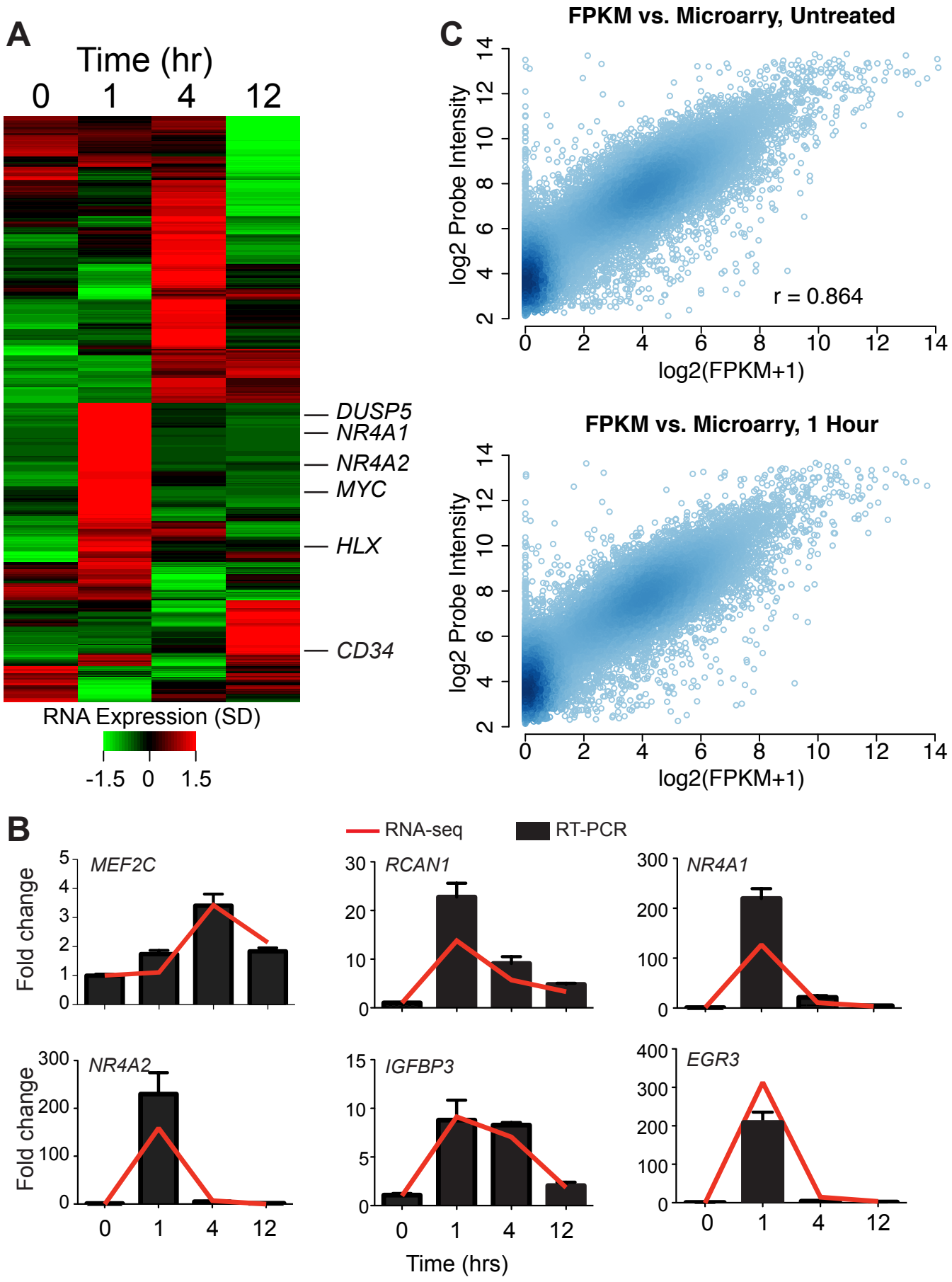


**Suppl. Fig. 8. RNA expression after VEGFA stimulation. A.** Hierarchically clustered heatmap of differentially expressed genes during VEGFA treatment of HUVEC cells. Several genes that were associated with dynamic H3K27ac loci that we studied are indicated. **B**. qRTPCR validation of differential gene expression following VEGFA treatment. **C**. Comparison of RNA-seq and published microarray RNA expression data (GSE15464 and GSE10778). Results were generally concordant between these methods. Pearson correlation coefficient is indicated.

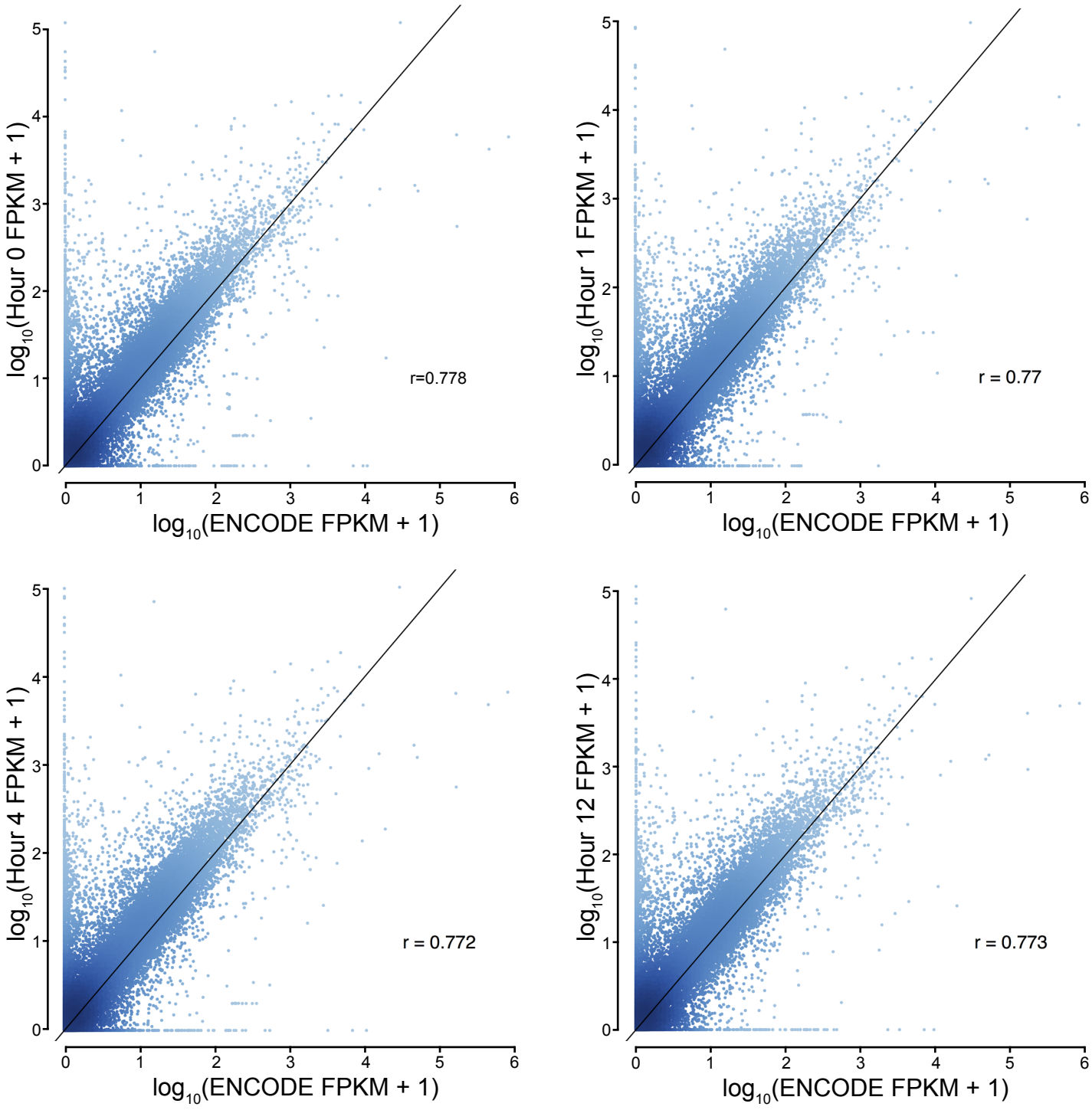


**Suppl. Fig. 12. RNA-seq measurement of HUVEC gene expression during VEGFA stimulation, compared to ENCODE data in full endothelial growth media.** Y-axis indicates data from this study, obtained after 12 hours of growth factor and serum withdrawl, followed by VEGFA treatment for 0, 1, 4, or 12 hours. X-axis indicates the ENCODE HUVEC data. r is the Spearman correlation coefficient for the unfiltered data.

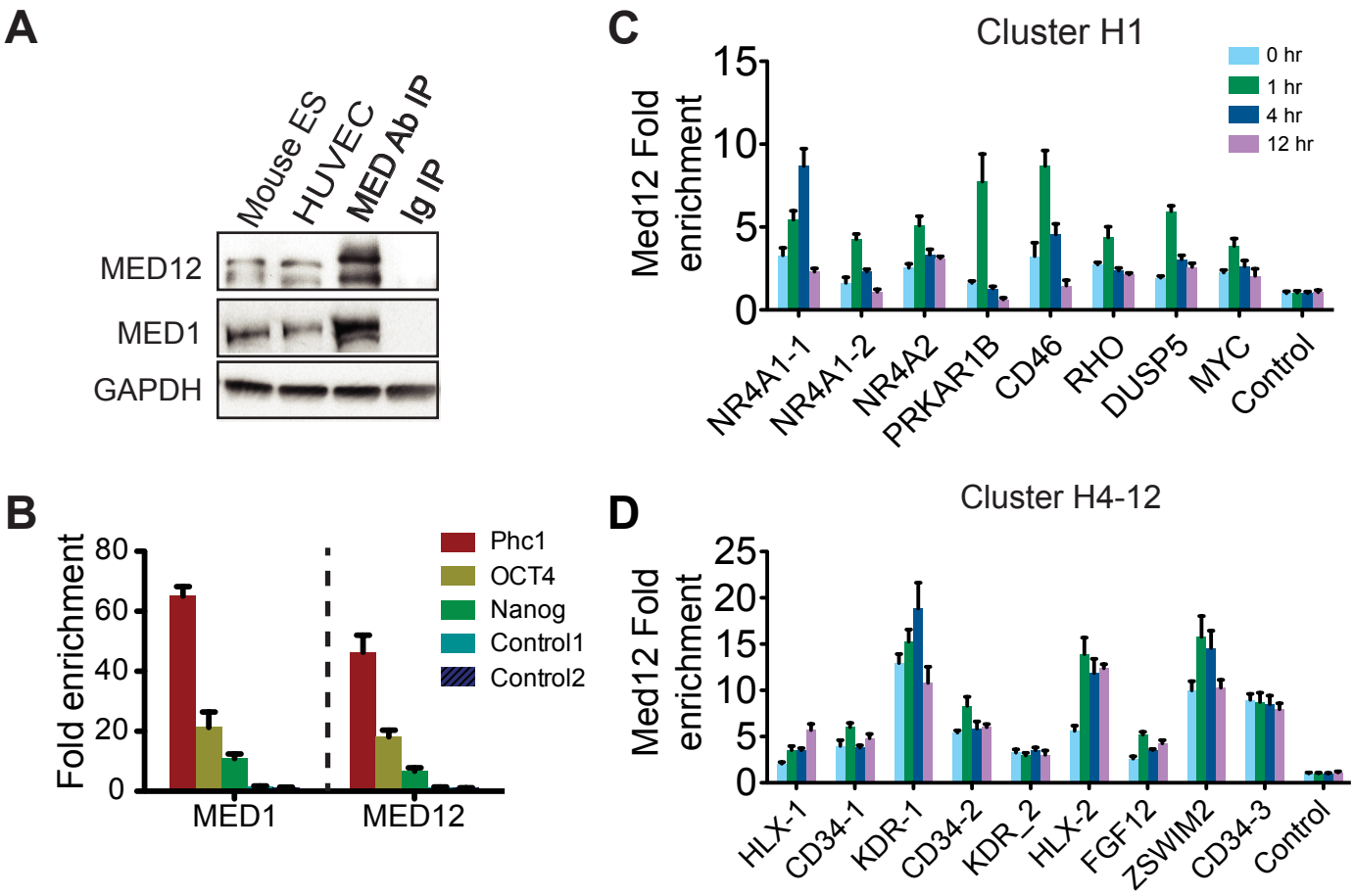


**Suppl. Fig. 13. RNA expression and Mediator chromatin occupancy after VEGFA stimulation. A**. Mediator 1 and 12 (MED1 and MED12) expression in HUVEC cells. ES cells were used as control. Immunoprecipitation was performed with the corresponding MED antibody. MED1 and MED12 expression in HUVEC was equivalent to ES cells. **B**. Chip-qPCR validating the specificity and affinity of MED1 and MED12 antibodies in ChIP using previously reported loci in mouse embryonic stem cells. **C-D**. MED12 Chip-qPCR of H3K27ac dynamic sites belonging to the H1 or H4-12 clusters. VEGFA stimulated MED12 occupancy of H3K27ac dynamic loci.